

# Lithium Borohydride (LiBH<sub>4</sub>): An Innovative Material for Neutron Radiation Shielding

M. Lotfalian<sup>a</sup>, M. Athari Allaf<sup>a,\*</sup> AND M. Mansouri<sup>a</sup>

<sup>a</sup>Islamic Azad University, Science and Research Branch, Department of Nuclear Engineering,  
1477893855 Tehran, Iran

\*e-mail: [athari@srbiau.ac.ir](mailto:athari@srbiau.ac.ir)

## Abstract

Radiation shielding plays a crucial role in various industries, including nuclear and space exploration. Among the most abundant elements and isotopes found in nature, <sup>10</sup>B has one of the highest neutron absorption cross-sections, closely followed by <sup>6</sup>Li. It is worth noting that hydrogen, with its light nucleus, serves as an excellent neutron reflector. Surprisingly, the potential of the lithium borohydride molecule (LiBH<sub>4</sub>), which consists exclusively of these elements, as a shield against neutron radiation has not yet been explored.

This study investigates various materials that can potentially be used as shields. First, we assessed traditional shields and previous optimizations for shielding. The findings showed that concrete containing 10% B<sub>4</sub>C yielded the best results. High-performance concrete (HPC) replaced regular concrete. By gradually incorporating lithium borohydride into the shield, along with the appropriate level of boron carbide, further optimization was achieved. Calculations were performed using the MCNPX 2.7E code.

The introduction of the new shield resulted in a significant 40% reduction in volume compared with the previous sample. The study findings showed that a 30 cm thick shield effectively blocked 95% of the total neutrons and 92% of the total gamma radiation. Additionally, it was noted that the shielding effects of lithium borohydride against fast neutrons are greater than those of boron carbide. Various parameters and data of the designed shield were calculated and compared with those of the previous sample.

**KEYWORDS:** radiation shielding optimization, lithium borohydride, high performance concrete

## 1. Introduction

Safety and health have always been primary concerns, leading researchers to continuously develop nuclear shielding materials for several decades. However, limitations in volume and transportation of these shields have prompted researchers to explore alternative materials. It is predicted that in the future, there will be a greater focus on newer and more accessible materials that occupy less space.

One such material is high performance concrete (HPC), which can be produced using conventional materials and processes. In addition, neutron shielding requires the use of boron and lithium hydride (LiH) as filler materials. Specifically, natural boron consists of 19.8% of <sup>10</sup>B and lithium consists of 7.59% of <sup>6</sup>Li. By evaluating and selecting the most suitable shield on the basis of previous optimizations (concrete containing boron carbide), significant results can be achieved by replacing conventional concrete with HPC and gradually adding the new compound Lithium Borohydride (LiBH<sub>4</sub>). The new compounds can be used in the future in industries that work with neutron beams, such as those related to nuclear fusion or accelerators.

Considerable research has already been conducted on shield optimization. Some researchers have focused on optimizing the proportion of metals in the alloy, whereas others have explored the use of fillers in concrete or polyethylene.

A study was conducted to develop HPC samples that are both mechanically strong and durable. This study focused on analyzing the mechanical properties, crack resistance, sulfate attack resistance, frost resistance, and impermeability of concrete with various mineral admixtures, specifically mineral powder and fly ash. Moreover, considering the aspect of sustainability and

future trends in the advancement of high-performance computing (HPC) will offer a more holistic outlook within this domain [1].

Findings from an investigation showed that high concentrations of tungsten oxide ( $\text{WO}_3$ ) in newly developed polymers can decrease their mean free path values. The results also indicated that the number of photons that penetrated depended on their energy [2].

In a study a composite shielding material was created using a hot-pressure sintering method. The material consisted of 10.00 wt% boron carbide particles ( $\text{B}_4\text{C}$ ), 13.64 wt% surface-modified cross-linked polyethylene (PE), and 76.36 wt% tungsten particles. The results demonstrated the composite's effectiveness in shielding high-energy neutrons. Simulation tests conducted in a white neutron field showed a remarkable 99.99% reduction in fast neutron penetration after a shielding thickness of 44 cm. Additionally, experimental results indicated a 99.70% decrease in neutron penetration [3].

In an innovative research project, researchers tested and studied the effect of  $\text{PbO-H}_3\text{BO}_3$  polymer nanoparticles in ordinary concrete. The results showed that nanoparticles performed better than microparticles in optimizing the shield against neutron radiation. Additionally, both modes improved the performance of the shield equally in terms of shielding against gamma radiation [4].

In a study on particle behavior, four commonly used algorithms (SCE, TLBO, DE, and GA) were used to optimize shield materials. The researchers concluded that the SCE algorithm performed the best. They then used this algorithm to optimize the shield compound and ultimately selected a multilayer composite [5].

In another study, the impact of tungsten oxide microparticles and nanoparticles on the concrete attenuation coefficient was investigated using the MCNPX2.4.0 code. The study found that adding  $\text{W}_3\text{O}$  microparticles, particularly  $\text{W}_3\text{O}$  nanoparticles, strengthened the shield against gamma rays [6].

In a separate study, the polyethylene compound was optimized for shielding against gamma and neutron beams by adding boron carbide and tungsten. The study concluded that adding 5 wt% of boron carbide to polyethylene effectively absorbed thermal neutrons, whereas adding 45 wt% of tungsten to polyethylene effectively absorbed gamma radiation [7].

In one study, an alloy made from different ratios of aluminum, iron, copper, and lead was tested against gamma rays. The compound containing 5% Al, 40% Fe, 50% Cu, and 5% Pb was selected as the optimal ratio after simulating four different ratios [8].

In another study, researchers analyzed different compounds of concrete and boron carbide as shields against gamma radiation. Numerical simulations demonstrated that adding boron carbide to concrete effectively enhanced its ability to shield against gamma radiation [9].

In a new and intriguing study, researchers analyzed specific hexaborides used as gamma radiation shields. The researchers experimentally synthesized the samples and then determined the chemical and physical characteristics of the manufactured samples. Ultimately, they concluded that the manufactured hexaborides show promising results compared with other gamma radiation shields that have been investigated in previous studies [10].

In a study, researchers examined concrete containing magnetite and limonite with different ratios as a shield against gamma rays. The study showed that adding limonite and, especially, magnetite, effectively improved the gamma attenuation coefficient of concrete [11].

In a new study, researchers investigated refractory high-entropy alloys as radiation shielding materials to evaluate various radiation attenuation parameters. These parameters include mass and linear attenuation coefficients, half-value layer, mean free path, effective atomic number, and buildup factors [12].

One study aimed to evaluate the shielding performance of ethylene propylene diene monomer (EPDM) rubber composites filled with 200 phr of different metal oxides (either  $\text{Al}_2\text{O}_3$ ,  $\text{CuO}$ ,  $\text{CdO}$ ,  $\text{Gd}_2\text{O}_3$ , or  $\text{Bi}_2\text{O}_3$ ) as protective materials against gamma and neutron radiations. For this purpose, different shielding parameters, including the linear attenuation coefficient ( $\mu$ ), mass attenuation coefficient ( $\mu/\rho$ ), mean free path (MFP), half value layer (HVL), and tenth value layer (TVL), were calculated. Based on  $\mu/\rho$  values, other significant shielding parameters such as the effective atomic number ( $Z_{\text{eff}}$ ), effective electron density ( $N_{\text{eff}}$ ), equivalent atomic number ( $Z_{\text{eq}}$ ), and exposure buildup factor (EBF) were also computed. This study demonstrates that the gamma-radiation shielding performance of the proposed metal oxide/EPDM rubber composites is increasing in the order of EPDM <  $\text{Al}_2\text{O}_3$ / EPDM <  $\text{CuO}$ / EPDM <  $\text{CdO}$ /EPDM <  $\text{Gd}_2\text{O}_3$ / EPDM <  $\text{Bi}_2\text{O}_3$ / EPDM. Furthermore, three sudden increases in the shielding capability in some composites occur at 0.0267 MeV for  $\text{CdO}$ /EPDM, 0.0502 MeV for  $\text{Gd}_2\text{O}_3$ / EPDM, and 0.0905 MeV for  $\text{Bi}_2\text{O}_3$ / EPDM composites [13].

The findings of the Radiation Assessment Detector (RAD) revealed that a journey to Mars would expose astronauts to a significant amount of harmful radiation. While previous robotic missions to Mars have not been successful, future human explorers heading to the Red Planet should be aware of the potential risks associated with radiation in deep space. The measurements obtained by the Curiosity rover during its voyage to Mars in August 2022 indicate that the impact of radiation on human space travelers remains a significant concern, although it is not yet fully understood [14].

A recent study introduced a superlattice nano-barrier-enhanced carbon fiber reinforced polymers (CFRPs) with a density of approximately 3.18 g/cm<sup>3</sup>. This innovative material seamlessly integrates with the mechanical properties of CFRP, effectively becoming a part of the composite structure. The research findings emphasize the necessity of both external and internal shielding mechanisms to safeguard satellites from trapped protons and electrons. Charged particles, such as protons with energies ranging from 0.1 to 400 MeV, are ensnared by the planet's robust magnetic field, forming radiation belts. These belts consist of an inner zone located between 6000 and 12,000 km altitude and an outer zone spanning from 25,000 to 45,000 km altitude, directly impacting satellites in orbit [15].

In one investigation, the use of celestite ( $\text{SrSO}_4$ ) minerals as aggregates in barrier composites was explored to ensure reliable handling in repositories, radiotherapy rooms, and research centers constructed with cement-based composites. The favorable shielding properties of celestite minerals make them ideal for this purpose. This study thoroughly examined the high-rate X-ray shielding ability and mechanical performance of the developed real radiation scenarios. In addition, the researchers found that the interface properties between the composite paste and celestite minerals remained compatible even when up to 30% of the celestite aggregate was replaced [16].

In the quest for the advancement of environmentally sustainable nuclear technology, scientists are discovering innovative ways to repurpose nuclear waste to create of biodiesel. Therefore, it is imperative to enhance radiation protection protocols in tandem with the evolution of nuclear technology [17].

In a recent study, researchers examined specific aspects of the interaction between gamma and neutron particles and DNA and RNA nucleobases, specifically adenine, cytosine, guanine, thymine, and uracil. The study focused on determining linear attenuation coefficient (LAC) values, which were then categorized based on energy ranges. Gamma ray penetration can be utilized at both the cellular and molecular levels. This categorization has the potential to improve the effectiveness of cancer cell eradication using radiation [18].

Researchers have recently conducted a study focusing on the significant effects of radioactive radiation on human health and the importance of radiation mapping. By using artificial neural networks trained with Monte Carlo data, they have developed a method to create high-resolution radiation maps. The researchers believe that this approach has the potential for practical implementation in real-world scenarios [19].

On the basis of the results of recent experimental and theoretical research, a series of simulation studies and calculations were conducted to determine the most suitable shield material. This involved the incorporation of various weight percentages of a new compound.

## 2. Materials and Methods

The research optimized a new single-layer shield without a moderator to protect against a wide spectrum of neutron-gamma mixed radiation, including fast neutrons. In contrast, fast reactors have a relatively hard spectrum, resulting in more neutrons escaping. Therefore, if we use a fast reactor as a source, more neutrons will interact with the shield. Additionally, using reactors as a source allows for time-dependent calculations to assess the shield's useful life. Consequently, the utilization of a fast reactor as a source is a favorable choice. Although the shield is being evaluated against a MET-1000 reactor, the objective is to design a radiation shield that can be applied in various scenarios. The source used is a fast reactor with a power of 1000 MWth containing a metal fuel known as MET-1000, as depicted in figure (1) [20]. The simulated reactor is a cylinder with a radius of 73.11 cm and a height of 85.82 cm. The overall density of the core was determined by averaging the volume ratios of its components. In addition, there is a 10 cm thick layer of HT-9 surrounding the reactor core, which acts as a reflector [9]. The reactor operates at full power under critical conditions, producing both neutrons and gamma rays. The simulation is conducted using the MCNPX 2.7E code. The calculations were performed using 100,000 neutron histories over a total of 200 cycles, which included 10 inactive cycles. The shield is simulated as a rectangular cube with dimensions of 5m×5m×5cm. It is positioned 50 cm from the source. A criterion for measuring flux changes is set up to 1 cm after the shield. Tables (I) and (II) present the ratios of the core and reflector compounds, respectively.

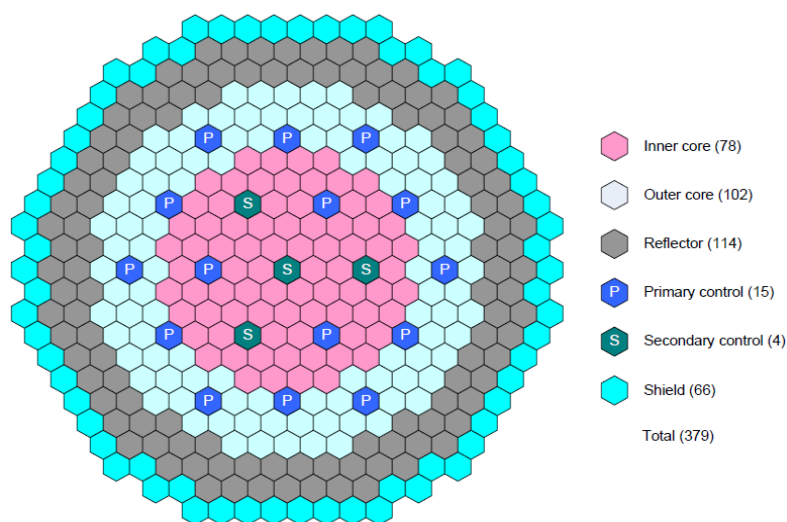


Figure 1. Radial layout of a MET-1000 core [20]

Table I. Ratio of ingredients in the core

Material	Na	<sup>239</sup> Pu	<sup>238</sup> U	<sup>235</sup> U	O	Fe	Ni	Cr	Mn	Mo	C	<sup>10</sup> B	<sup>11</sup> B
Ratio	0.353	0.0351	0.0809	0.0057	0.247	0.236	0.0013	0.0327	0.00145	0.00155	0.001	0.0012	0.0031

**Table II.** Ratio in ingredients of the reflector

Material	Si	Al	Fe	Ca	Mg	S	K	Na	Sr	O	H
Ratio	0.0259	0.00591	0.12625	0.145	0.00317	0.00691	0.00271	0.0192	0.00095	0.5085	0.1555

In the first step, we evaluated five different materials based on the results of other optimization studies. These materials included an optimal alloy consisting of 5 wt% lead, 40 wt% iron, 50 wt% copper, and 5 wt% aluminum [8]; concrete containing tungsten nanoparticles [6]; concrete containing 30wt% iron oxide [11]; polyethylene containing 5 wt% boron carbide and 45 wt% tungsten oxide [7]; and concrete containing an optimal amount of 10wt% boron carbide[9]. We also evaluated some conventional shields. After this evaluation, we selected concrete containing 10% boron carbide.

In the second step, we considered the use of 10% boron carbide in HPC. When space is limited, HPC can reduce the thickness of the shield structure without compromising its shielding effectiveness. We evaluated these compounds to further enhance the shield.

1- HPC containing 10% boron carbide

2- HPC containing 10% boron carbide and lithium borohydride (LiBH<sub>4</sub>).

We evaluated of the shields under identical physical and geometrical conditions, considering the realistic densities of the materials. The examined materials are listed in Table (III). Additionally, Tables (IV) and (V) display the weight ratios of concrete and polyethylene isotopes, respectively.

**Table III.** Compounds and elements studied in the first step

No.	name	Material
1	Without Shield	Without shield
2	PE	Polyethylene
3	Conc.	Ordinary concrete
4	HPC	High performance concrete
5	Pb	Pure lead
6	Pb, Al, Cu, Fe	A compound including 5% Al, 40% Fe, 50% Cu and 5% Pb [8]
7	PE, W <sub>3</sub> O, B <sub>4</sub> C	Polyethylene contains 5% B <sub>4</sub> C, 45% W <sub>3</sub> O [7]
8	Conc., Fe <sub>2</sub> O <sub>3</sub>	Concrete contains 30% Fe <sub>2</sub> O <sub>3</sub> [11]
9	Conc., W <sub>3</sub> O	Concrete contains tungsten nanoparticles [6]
10	Conc., B <sub>4</sub> C	Concrete contains 10% B <sub>4</sub> C [9]
11	HPC, B <sub>4</sub> C	High performance concrete contains 10% B <sub>4</sub> C
12	HPC, B <sub>4</sub> C, Li <sub>2</sub> O	High performance concrete contains 10% B <sub>4</sub> C, Li <sub>2</sub> O
13	HPC, B <sub>4</sub> C, LiBH <sub>4</sub>	High performance concrete contains 10% B <sub>4</sub> C, LiBH <sub>4</sub>

**Table IV.** Ratio of concrete isotopes [21]

No.	Element	Element weight fraction in concrete	Isotope natural abundance	Isotope weight percent in concrete
1	Si	0.337	<sup>28</sup> Si (92.27%) <sup>29</sup> Si (4.68%) <sup>30</sup> Si (3.05%)	<sup>28</sup> Si (31.1 %) <sup>29</sup> Si (01.58 %) <sup>30</sup> Si (01.03 %)
2	Al	0.337	<sup>27</sup> Al (4.68%)	<sup>27</sup> Al (3.4 %)
3	Fe	0.014	<sup>54</sup> Fe (5.84%) <sup>56</sup> Fe (91.68%) <sup>57</sup> Fe (2.17%) <sup>58</sup> Fe (0.31%)	<sup>54</sup> Fe (0.082 %) <sup>56</sup> Fe (1.28 %) <sup>57</sup> Fe (0.028 %) <sup>58</sup> Fe (0.00434 %)
4	Ca	0.044	<sup>40</sup> Ca (100%)	<sup>40</sup> Ca (4.4 %)
5	Na	0.029	<sup>23</sup> Na (100%)	<sup>23</sup> Na (2.9%)
6	O	0.532	<sup>16</sup> O (99.759%) <sup>17</sup> O (0.037%) <sup>18</sup> O (0.204%)	<sup>16</sup> O (53.07 %) <sup>17</sup> O (1.97 %) <sup>18</sup> O (10.85 %)
7	H	0.01	<sup>1</sup> H (≈ 100%)	<sup>1</sup> H (1 %)
Total		1.00		

**Table V.** Ratio of polyethylene isotopes [21]

No	Element	Weight fraction in polyethylene	Isotope natural abundance	Isotope weight percent in polyethylene
1	Hydrogen	0.143	$^1\text{H}$ ( $\approx 100\%$ )	$^1\text{H}$ ( $\approx 14.3\%$ )
2	Carbon	0.857	$^{12}\text{C}$ (98.89%) $^{13}\text{C}$ (1.11%)	$^{12}\text{C}$ (84.75%) $^{13}\text{C}$ (0.95%)
	Total	1.00	-	1.00

### 3. Calculations and Discussion

#### 3.1. Benchmark Results

To validate the simulated source, the neutron spectrum and  $K_{\text{eff}}$  were compared with those of the MET-1000 reactor. The  $K_{\text{eff}}$  of the simulated reactor was calculated to be 1.02, which is less than 1% different from the value given in the reference model [20]. The spectrum was found to be identical to that of the reference sample, and the average neutron flux in the core was determined to be  $1.42 \times 10^{15}$  n/cm<sup>2</sup>. Figure (2) shows a comparison between the neutron spectra calculated in the MET-1000 reactor and those in reference [22].

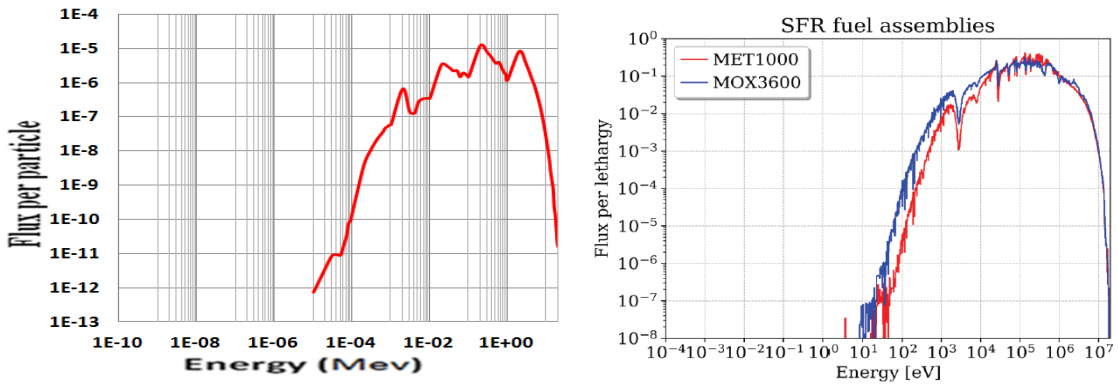


**Figure 2.** Comparison between the neutron spectra calculated in the simulated MET-1000 reactor (left side) and the main reference [22] (right side)

The standard deviation was calculated to be approximately 0.1 %. Because the computation of  $K_{\text{eff}}$  and the chain reactions depend on the rest of the parameters, the standard deviation also applies to them.

#### 3.2. Evaluation of Shields against Neutron Radiation

The average flux after passing through the 5 cm thick shield is shown in Figure (3). The graphs are organized on the basis of the materials' effectiveness in reducing flux. The lowest neutron flux was observed when using HPC containing boron carbide. The neutron spectrum after passing through the three different materials is shown in Figure (4).

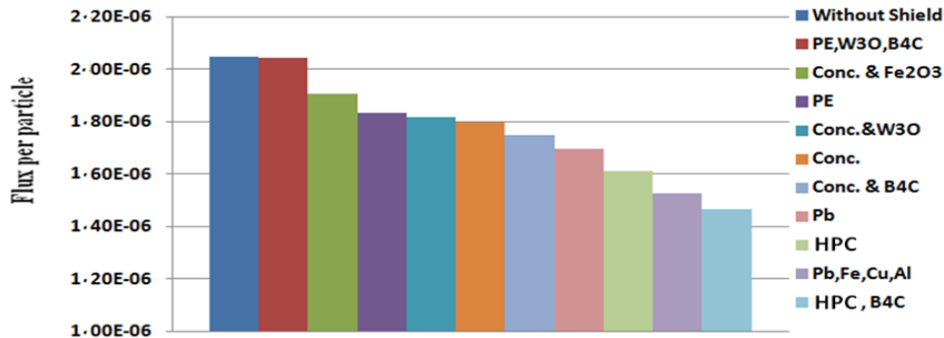


**Figure 3.** Total neutron flux after different types of shields with a thickness of 5 cm

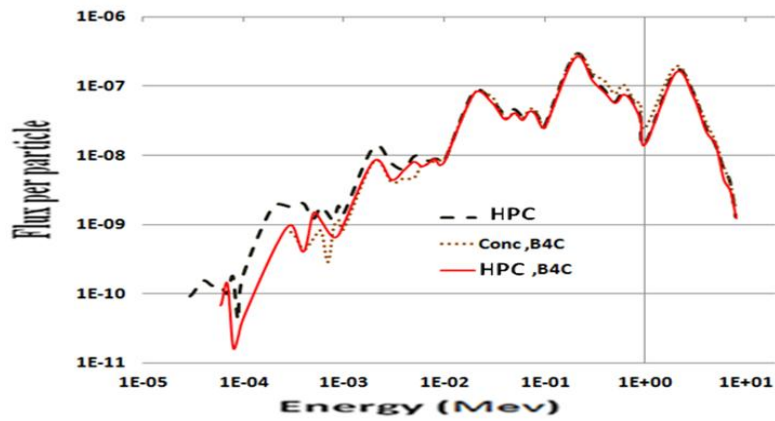


**Figure 4.** Neutron spectrum after three different materials with a thickness of 5 cm

As can be concluded from the graph, the addition of boron carbide is more effective for low-energy neutrons (below 10 keV).

### 3. 3. Evaluation of Shields against Gamma Radiation

The results for all types of shields against gamma radiation are shown in Figure (5). The gamma spectrum after three layers of shielding is shown in Figure (6).

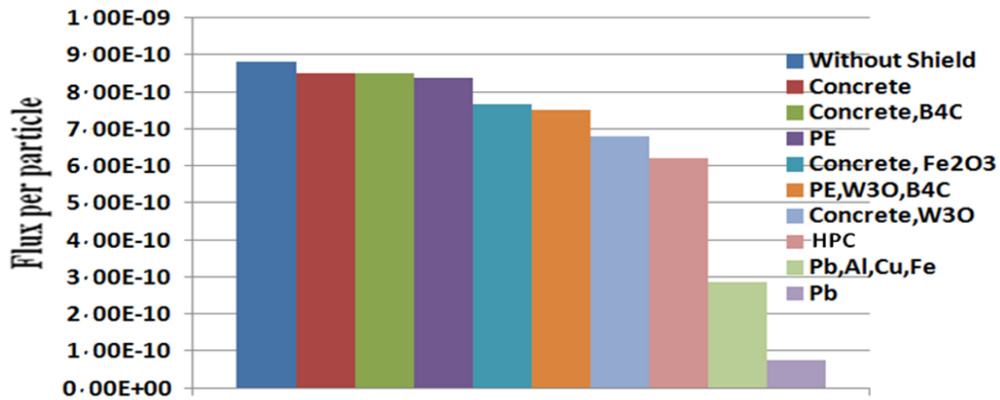


**Figure 5.** Total gamma flux after using different types of shields with a thickness of 5 cm

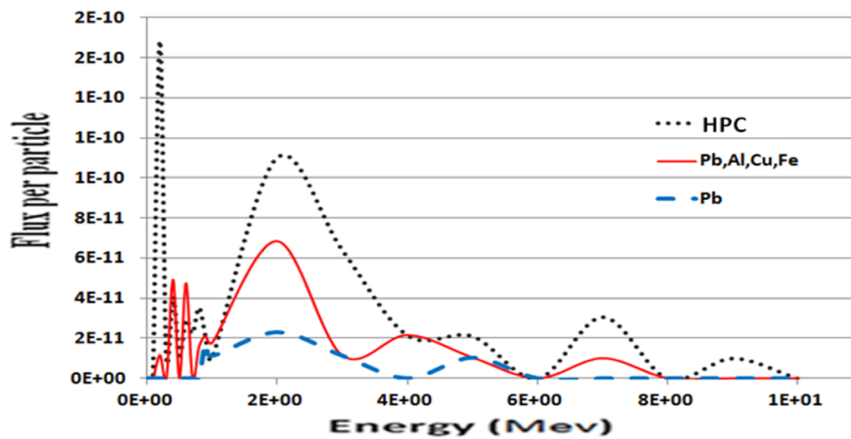


**Figure 6.** Gamma spectrum after passing through three different materials with a thickness of 5 cm

Although the total gamma flux after the shields was not equal, the intended shields effectively attenuated the gamma rays and exhibited similar fluctuations in relation to the spectrum. Different shields do not equally reflect neutrons; therefore, the ratio of neutron flux after and before the shields is not a suitable criterion for comparison. The main criterion for a shield is the flux rate after the shield. Tungsten-containing shields have a relatively positive impact on the effectiveness of gamma shields. However, the reactions  $^{182}\text{W}(n,2n)^{181}\text{W}$ ,  $^{186}\text{W}(n,2n)^{185}\text{W}$ , and  $^{186}\text{W}(n,3n)^{184}\text{W}$  [23] showed poor performance against fast neutrons.

### 3. 4. Behavior of High Performance Concrete and Lithium Borohydride ( $\text{LiBH}_4$ )

High-performance concrete: This type of concrete has superior strength and long-term performance. The typical composition of a proprietary HPC mix can be seen in table (VI) [24].

**Table VI.** Composition of the HPC mix [24]

HPC		OC	
Component	[kg/m <sup>3</sup> ]	Component	[kg/m <sup>3</sup> ]
Technical sand	979	Sands	1150
cement I 42.5R	693	Cement CEM II/B-M (S-LL) 32,5	360
quartz flour	332	gravel	810
Silica fume	178	-	-
superplasticizer	29.6	superplasticizer	2.7
water	174	water	155
total	2385.6	total	2477.7

New compounds can be designed to enhance the effectiveness of shields. Therefore, we decided to study lithium compounds. Among the range of chemicals containing lithium, we selected lithium borohydride ( $\text{LiBH}_4$ ) as our compound of choice. This is because each molecule of  $\text{LiBH}_4$  contains one boron atom (which acts as an absorber) and four hydrogen atoms (which act as moderators). In addition, lithium borohydride is readily available. Our results showed that, even when using the optimized amount of boron carbide in the shield compound, the addition of lithium borohydride led to a significant exponential increase in the shield's effectiveness. To determine the optimal value of  $\text{LiBH}_4$ , we added different proportions of  $\text{LiBH}_4$  to HPC that already contained boron carbide.

To determine the optimal content of lithium borohydride, we evaluated various percentages of  $\text{LiBH}_4$  with different shield thicknesses. As shown in figure (7), the neutron flux decreased as the percentage of lithium borohydride in the shield increased.

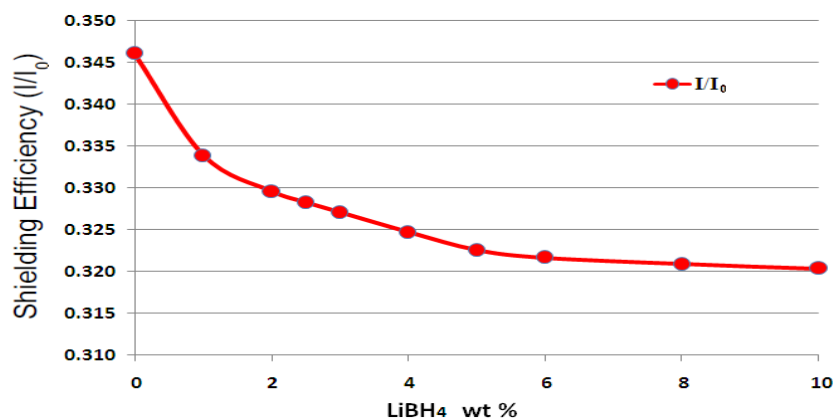


**Figure 7.** Variation of neutron flux relative to  $\text{LiBH}_4$  content in the HPC shield containing 10%  $\text{B}_4\text{C}$  and 5cm thickness: The neutron flux decreases again after the shield by increasing the  $\text{LiBH}_4$  content.

The bar chart in Figure (8) shows that the total neutron flux is lower after passing through the new shields compared with the previous shields. The spectra of the six shields at different thicknesses (5, 10, 15, and 20 cm) are shown in figure (9).

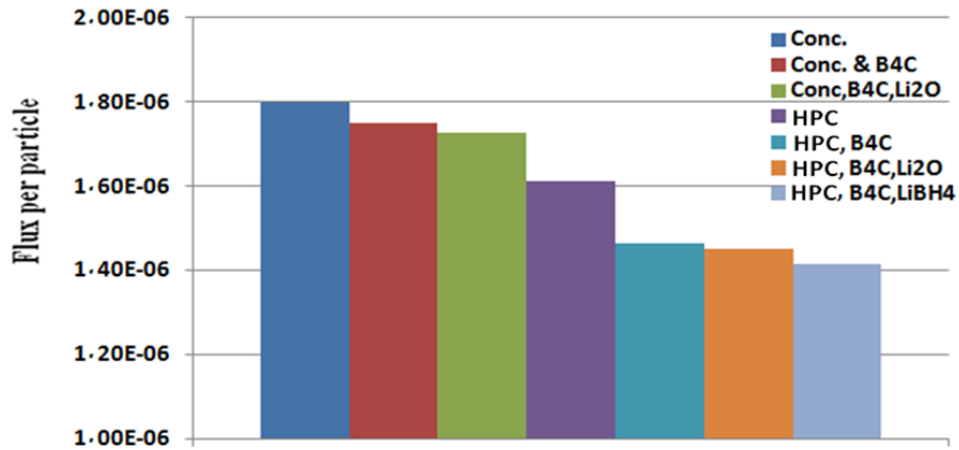


Figure 8. Comparison of the calculated neutron flux after passing through new and conventional shields

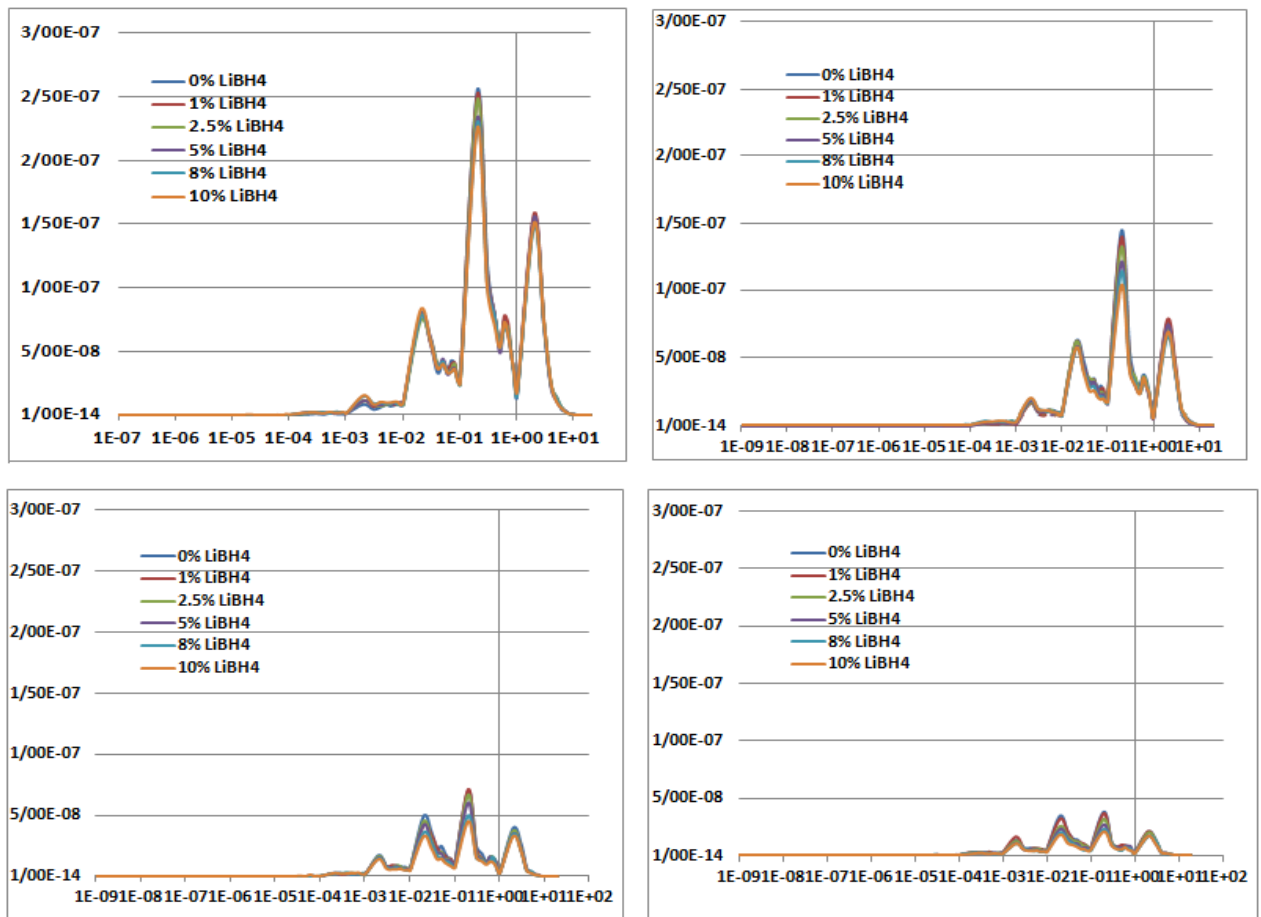
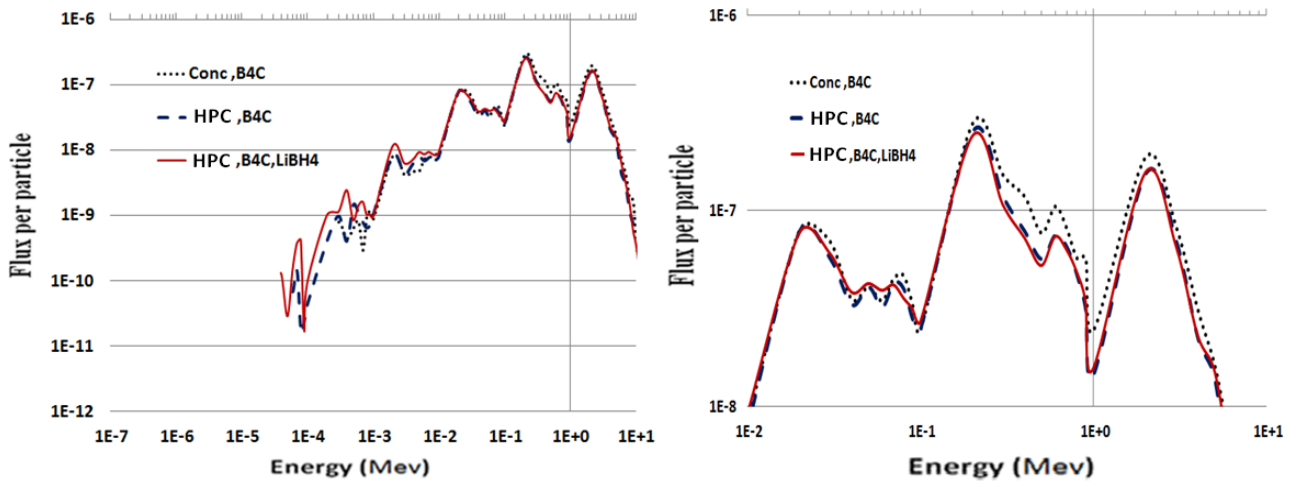


Figure 9. Spectra of neutrons passing through shields with varying thicknesses (5, 10, 15, and 20 cm) and different weight percentages of LiBH<sub>4</sub>

The transfer of neutron radiation can be classified into three types of shields based on the neutron spectrum. Figure (10) shows the results.



**Figure 10.** Two magnifications of the neutron spectrum after three types of shields with a thickness of 5 cm

As can be concluded from the graph, the addition of  $\text{LiBH}_4$  is more effective in preventing neutrons in the energy range of 100 keV to 1 MeV.

In addition, the transmission ratio of gamma radiation through three main types of shields was classified in terms of the gamma spectrum in two regions. Figure (11) shows the results.

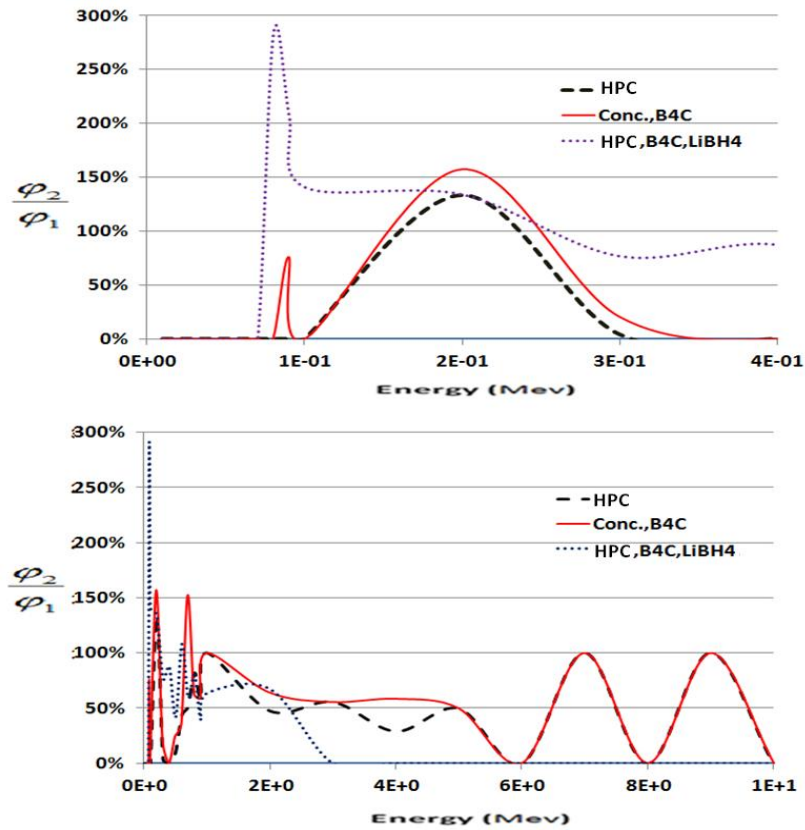


**Figure 11.** The ratio of passing gamma radiation before and after the thickness of 5cm of three types of shields as a function of the gamma spectrum, which is classified into two energy groups ( $\varphi_1$  is the gamma flux before the shield and  $\varphi_2$  is the gamma flux after the shield).

The amount and range of gamma radiation passing through the shield are determined not only by density but also by the effectiveness of fillers such as B<sub>4</sub>C and LiBH<sub>4</sub>. The role of density is certainly significant. HPC responded better to gamma radiation than ordinary concrete. The effect of fillers containing elements such as boron and lithium on electromagnetic waves has already been investigated. [25]

### 3. 5. Calculation of other parameters

The half-layer thickness, total cross-section, and linear attenuation coefficient of the designed shield against gamma and neutrons are shown in Tables (VII) and (VIII), respectively.

**Table VII.** Calculated data for several shields against neutron radiation

Material	$\Sigma_t$ (1/cm)	Half layer value (cm)	$\lambda$ (cm)
HPC, B <sub>4</sub> C , LiBH <sub>4</sub>	2.09E-01	3.32	4.79E+00
Conc.,B <sub>4</sub> C	1.55E-01	4.471	6.46E+00

**Table VIII.** Calculated data for several shields against gamma radiation

Material	$\Sigma_t$ (1/cm)	Half layer value (cm)	$\lambda$ (cm)
HPC, B <sub>4</sub> C , LiBH <sub>4</sub>	2.81E-01	2.47	3.56E+00
Pb	1.31E+00	0.53	7.66E-01

Table (IX) presents the neutron and gamma flux results obtained from the evaluation of the key shielding materials used in this study.

**Table IX.** Calculated neutron and gamma fluxes per particle after 5 cm thickness of various shields

Material	Neutron flux after 5cm thick of Shield	Gamma flux after 5cm thick of Shield
Conc.&W <sub>3</sub> O [6]	1.82E-06	6.81E-10
PE,W <sub>3</sub> O,B <sub>4</sub> C [7]	2.05E-06	7. 5E-10
Pb,Fe,Cu,Al [8]	1.53E-06	2.85E-10
Conc. & B <sub>4</sub> C [9]	1.75E-06	8.5E-10
Conc. & Fe <sub>2</sub> O <sub>3</sub> [11]	1.91E-06	7.67E-10
Pb	1.70E-06	7.39E-11
HPC	1.61E-06	6.20E-10
HPC, B <sub>4</sub> C	1.47E-06	6.04E-10
HPC, B <sub>4</sub> C, Li <sub>2</sub> O	1.43E-06	6.01E-10
HPC, B <sub>4</sub> C, LiBH <sub>4</sub>	1.41E-06	5.97E-10

As expected, the designed shield performed better against neutrons than the concrete containing boron carbide. However, the results indicate that the lead shield is more effective against gamma radiation. It is important to determine if the optimal thickness of the shield against neutron radiation also provides satisfactory results against gamma radiation. Therefore, the thickness of the shield against neutrons should be optimized first.

### 3.6. Shield thickness optimization

The difference in flux becomes more apparent as the thickness of the shield increases, highlighting the varying effects of different types of shields. To assess this, several shields were

tested with an incremental increase in thickness. The neutron flux alterations after passing through the four materials of different thicknesses are illustrated in Figure (12).

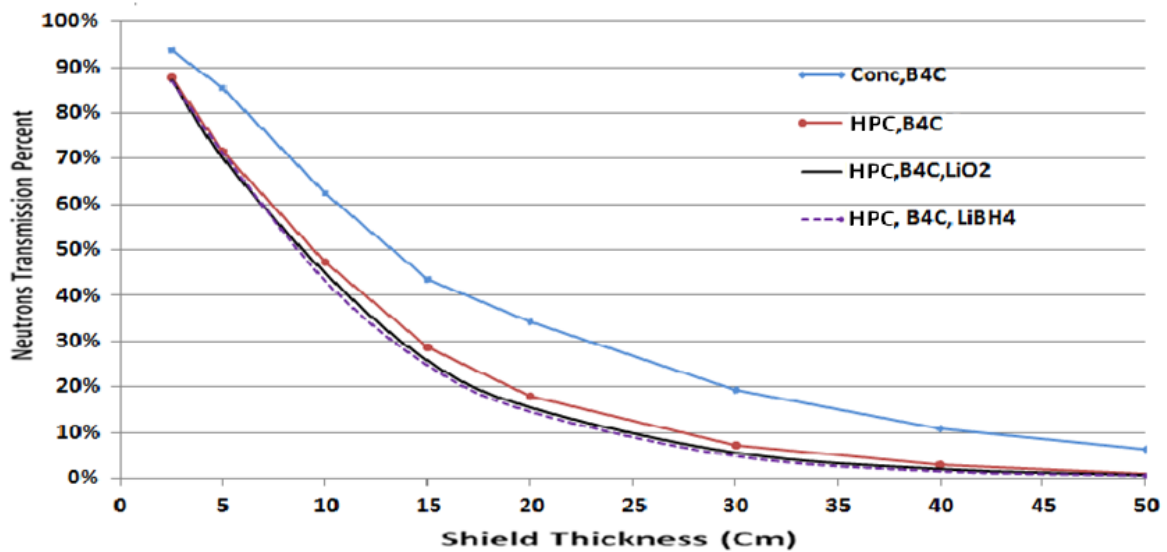


Figure 12. Changes in neutron flux relative to variations in shield thickness.

The effect of the material change increases with thickness. For instance, if we want 10% of the neutron flux to pass through, we would need a thickness of approximately 25 cm of HPC that includes B<sub>4</sub>C (boron carbide) and LiBH<sub>4</sub> (lithium borohydride). On the other hand, 40 cm of regular concrete containing boron carbide would be necessary. This represents a 40% reduction in the thickness. Moreover, increasing the thickness of HPC containing 10% B<sub>4</sub>C and 5% LiBH<sub>4</sub> by more than 30 cm has a minimal effect. Therefore, we can conclude that the optimal thickness for this shield is 30 cm.

### 3.7. Effect of Monolayer Shielding Against Gamma Rays

In this step, we calculated the value of the gamma flux after optimizing the shield and compared it with previous measurements, as shown in Figure (13). The figure shows that although the total gamma flux after implementing the new shield is not lower than that of all previous shields (especially when compared to lead), its performance is satisfactory. Figure (14) illustrates the changes in the gamma flux with an increase in the shield thickness.

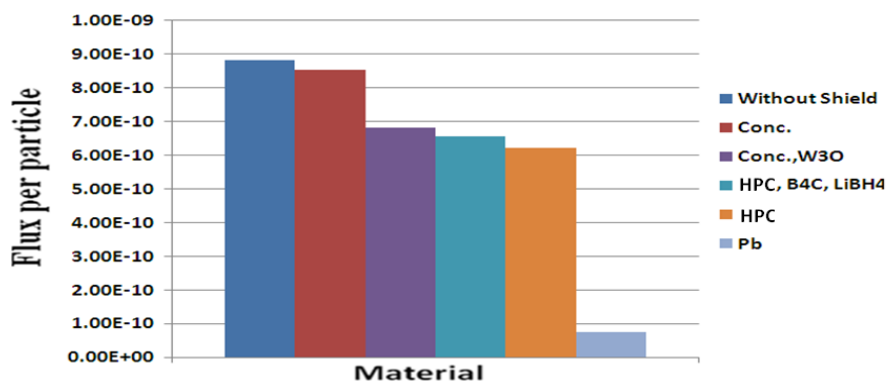
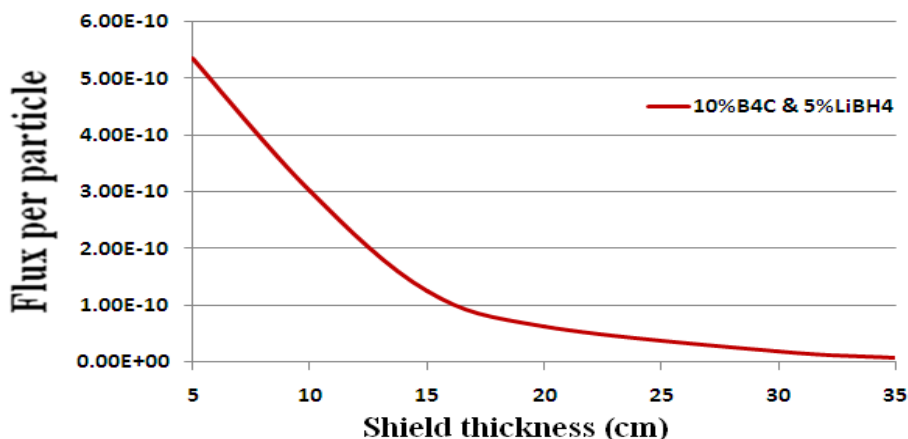


Figure 13. Comparison of gamma flux after the new shield and some previous shields



**Figure 14.** Changes in gamma flux after shielding relative to a gradual increase in shield thickness

Now, let's consider the optimal thickness of the shield, which is made of concrete containing boron carbide and  $\text{LiBH}_4$ , against neutron radiation. It has been observed that a shield with a thickness of 30 cm can prevent more than 92% of the total gamma radiation. The calculation was also repeated for a shield with a thickness of 35 cm, and it was found that a 35 cm thick shield completely blocks the passage of gamma radiation. Calculations show that if this type of shield is used with a thickness of 30 cm or more, there is no need to use lead as a second layer for gamma shielding. Additional calculations were conducted for the shield using various thicknesses, and it was determined that altering the weight percentage of lithium borohydride had no impact on the gamma attenuation coefficient.

Recent findings suggest that, in addition to increasing density, various intriguing factors can also play a role in enhancing the efficacy of a gamma shield. It is currently understood that melanin in the skin has the ability to provide protection against radiation through its interaction with electromagnetic radiation [25].

This protective mechanism can also be facilitated by distinct chemical reactions that have been demonstrated through artificial modeling.

### 3. 8. Shield Quality over Time

The interaction between the neutrons and shield materials can have a significant impact, even at low levels. Therefore, it is necessary to calculate the consumption of the main neutron absorber isotopes when optimizing new shields under various conditions. However, if a shield is positioned close to a powerful source, such as the Met-1000 reactor, the flux inside the shield cannot be ignored. To assess the production of hazardous isotopes resulting from the interaction between the shield and neutrons, time-dependent calculations are helpful.

To evaluate the lifespan of a concrete shield containing 10% boron carbide and 5%  $\text{LiBH}_4$  with a thickness of 30 cm, the quality of the shield was assessed for 180 days after the reactor reached full power. Time-dependent calculations were performed using the BURN card to determine the reduction amount of  $^{10}\text{B}$  and  $^6\text{Li}$ , which are the main absorbers. The results are presented in Table (X).

**Table X.** Changes (consumption) in adsorbent isotopes in the shield over time

Time (days)	$^{10}\text{B}$ (gr)	$^6\text{Li}$ (gr)
0	1.242E+05	3.711E+03
80	1.240E+05	3.710E+03
180	1.238E+05	3.709E+03

Although the neutron flux inside the shield is low, some absorbing isotopes, such as  $^{10}\text{B}$  and  $^6\text{Li}$ , have reacted with neutrons and decreased. The consumption of  $^{10}\text{B}$  and  $^6\text{Li}$  after 180 days, compared with their initial values, was 0.32% and 0.054%, respectively.

#### 4. Conclusions

In this study, various shields were studied against a wide spectrum of neutron-gamma mixed fields. We evaluated different conventional shields and considered the optimized results from previous studies as potential shielding materials. The primary results showed that concrete containing 10% wt of boron carbide provided the best performance against neutron radiation. We replaced the HPC with ordinary concrete and observed an improvement in shield quality by gradually adding lithium borohydride. This improvement occurred even with the optimal concentration of 10 wt% of boron carbide in the shield compound.

The optimal weight percentage of lithium borohydride in the designed shield was determined to be 5 wt%. Under these conditions, the new shielding material (HPC containing 10%  $\text{B}_4\text{C}$  and 5%  $\text{LiBH}_4$ ) could reduce the volume by 40.0% compared with concrete containing boron carbide. Adding boron carbide is more effective for low-energy neutrons (below 10 keV), whereas adding  $\text{LiBH}_4$  is more effective for neutrons in the energy range of 100 keV to 1 MeV. As neutrons pass through the shield, many fast neutrons are converted into thermal neutrons, causing their energy to decrease and resulting in an increase in the absorption cross-section. In such cases, a moderator is often unnecessary. Because the source is a fast reactor, it contains a high percentage of fast neutrons. Lithium borohydride was found to be more effective than boron carbide as a shield against fast neutrons. Therefore, when these neutrons pass through a shield containing light elements, they become thermal neutrons. In this way, the microscopic capture cross-section of absorption increases over the entire shield composition. However, including fillers such as  $\text{B}_4\text{C}$  and  $\text{LiBH}_4$  can significantly enhance shielding effectiveness. Although HPC containing  $\text{B}_4\text{C}$  and  $\text{LiBH}_4$  was effective against neutrons, a shield thickness of 30 cm prevented 95% of the total neutron spectrum and 92% of the total gamma spectrum. Therefore, by gradually increasing the shield's thickness to 30 cm or more, there is no need for a second layer of the shield to protect against gamma radiation.

Despite the significant increase in shield quality achieved by incorporating compounds containing neutron-absorbing isotopes like  $^{10}\text{B}$  and  $^6\text{Li}$ , the depletion of these isotopes was very low. After 180 days of full power reactor operation, it was found that only 0.32% of  $^{10}\text{B}$  and 0.054% of  $^6\text{Li}$  were consumed. This indicates that the quality of the shield remained nearly constant over time, and its useful life is expected to be long.

Lithium borohydride exhibits promising properties for neutron radiation shielding and has the potential for novel applications and optimization. Furthermore,  $\text{LiBH}_4$  offers potential for optimization and customization. This adaptability opens doors for tailoring  $\text{LiBH}_4$  to specific applications, ensuring optimal radiation shielding performance.

#### References

- [1] Yongguang Han and Tianhua Zhou, "Performance Analysis of High-Performance Concrete Materials in Civil Construction", *Materials*, August 2023
- [2] Mohamed Elsafi, Nouf Almousa, Nuha Al-Harbi, M.N. Almutiri, Sabina Yasmin, M.I. Sayyed, "Ecofriendly and radiation shielding properties of newly developed epoxy with waste marble and  $\text{WO}_3$  nanoparticles", *Journal of Materials Research and Technology*, Volume 22, January-February 2023

- [3] Qiankun Shao, Qingjun Zhu, Yuling Wang, Shaobao Kuang, Jie Bao, Songlin Liu, "Development and application analysis of high-energy neutron radiation shielding materials from tungsten boron polyethylene", *Nuclear Engineering and Technology*, January 2024
- [4] K. Mokhtari, M. Kheradmand Saadi, H. Ahmad Panahi, Gh Jahanfarnia, "The shielding properties of the ordinary concrete reinforced with innovative nano polymer particles containing  $PbO-H_3BO_3$  for dual protection against gamma and neutron radiations", *Radiation Physics and Chemistry*, Volume 189, December 2021
- [5] Yao Cai, Huasi Hu, Ziheng Pan, Weiqiang Sun, Mingfei Yan, "Metaheuristic optimization in shielding design for neutrons and gamma rays reducing dose equivalent as much as possible", *Annals of Nuclear Energy*, Volume 120, 2018
- [6] H.O. Tekin, V.P. Singh, T. Manici, "Effects of micro-sized and nano sized  $WO_3$  on mass attenuation coefficients of concrete by using MCNPX code", *Applied Radiation and Isotopes*, Volume 121, March 2017
- [7] M. Salimi, N. Ghal-Eh, E. Asadi Amirabadi, "Characterization of a new shielding rubber for use in neutron-gamma mixed fields", *Nuclear Science and Techniques*, Volume 29, 2018
- [8] S. M. Reda, "Gamma Ray Shielding by a New Combination of Aluminum, Iron, Copper and Lead Using MCNP5", *Arab Journal of Nuclear Science and Applications*, 2016
- [9] Srboľjub J. Stankovic, Radovan Ilic, Ksenija Janković, Ksenija Janković, Boris Loncar, "Gamma Radiation Absorption Characteristics of Concrete with Components of Different Type Materials", *Acta Physica Polonica A*, Volume 117, May 2010
- [10] Hasan Gulbicim, Mecit Aksu, Nureddin Turkan, Cansu Babuz, "Gamma ray shielding properties of synthesized lanthanide borides using EGSnrc code", *Nuclear Instruments & Methods in Physics Research Section B: Beam Interactions with Materials and Atoms*, Volume 542, September 2023
- [11] Aycan Gur, Birol Artig, Tahir Cakir, "Photon Attenuation Properties of Concretes Containing Magnetite and Limonite Ores", *Physicochemical Problems of Mineral Processing*, Volume 53, 2017
- [12] Z. Aygun, "Study on Radiation Shielding Characteristics of Refractory High Entropy Alloys by EpiXS Code", *Acta Physica Polonica A*, Vol. 143, 2023
- [13] Mahmoud T. Alabsy, Mohamed Abd Elzaher, "Radiation shielding performance of metal oxides/EPDM rubber composites using Geant4 simulation and computational study", *Scientific Reports*, May 2023
- [14] Rechar A. Kerr, "Radiation Will Make Astronauts' Trip to Mars Even Riskier", *Science*, Volume 340, Issue 6136, 31 May 2013
- [15] Michal Delkowski, Christopher T G Smith, José V Anguita, S Ravi P Silva , "Radiation and electrostatic resistance for ultra-stable polymer composites reinforced with carbon fibers" *Science Advances*, Volume 9, Issue 11, March 2023
- [16] Oğuzhan Öztürk, Şeyma Nur Karaburç, Murat Saydan, Ülkü Sultan Keskin, "High rate X-ray radiation shielding ability of cement-based composites incorporating strontium sulfate ( $SrSO_4$ ) minerals", *kerntechnik*, February 2022
- [17] Christopher Selvam D., Yuvarajan Devarajan, Raja T., "Study on analysing the potential benefits of utilizing nuclear waste for biodiesel production", *Kerntechnik*, Volume 89, April 2024

- [18] G.B Hiremath, V.P. Singh, P.N Patil, N.H Ayachit, N.M Badiger, “Attenuation Properties of DNA Nucleobases Against Nuclear Radiation Using EpiXS, Py-MLBUF, and NGCal Software”, *Acta Physica Polonica A*, Volume 145, April 2024
- [19] Ryotaro Okabe, Shangjie Xue, Jayson R. Vavrek, et al., ” Tetris-inspired detector with neural network for radiation mapping”, *Nature Communications*, April 2024
- [20] Nuclear Science Committee, "Benchmark for Neutronic Analysis of Sodium-cooled Fast Reactor Cores with Various Fuel Types and Core Sizes", OECD Nuclear Energy Agency, February 2016
- [21] Harmon, C. D., Busch, R. D., Briesmeister, J. F., Forster, R. A., "Criticality Calculations with MCNP5<sup>TM</sup>: A Primer", Los Alamos National Laboratory", World Wide Web release, January 2009
- [22] Friederike Bostelmann, Andrew M. Holcomb, Justin B. Clarity, William J. Marshall, Vladimir Sobes, Bradley T. Rearden "Nuclear Data Performance Assessments for advanced reactors", Oak Ridge National Laboratory, March 2019
- [23] A.Yu. Konobeyev, U. Fischer, D. Leichtle, P.E. Pereslavl'tsev, S.P. Simakov, "Evaluated data files for neutron irradiation of <sup>182</sup>W and <sup>186</sup>W at energies up to 200MeV", Institute for Neutron Physics and Reactor Technology, Karlsruhe institute of technology, 2019
- [24] Lenka Laiblová, Jan Pešta, Anuj Kumar, Petr Hájek, Ctislav Fiala, Tomáš Vlach, Vladimír Koččí, “Environmental Impact of Textile Reinforced Concrete Facades Compared to Conventional Solutions—LCA Case Study”, *Materials*, September 2019
- [25] N Yıldız Yorgun, E Kavaz, H O Tekin, M I Sayyed, Ö F Özdemir, "Borax effect on gamma and neutron shielding features of lithium borate glasses: an experimental and Monte Carlo studies", *Materials Research Express*, Volume 6, November 2019
- [26] Wanjie Xie, Ali Dhinojwala, Nathan C Gianneschi and Matthew D Shawkey, “Interactions of Melanin with Electromagnetic Radiation: From Fundamentals to Applications”, *Chemical Reviews*, May 2024